THERMAL PROPERTIES OF GREEN POLYMERS AND BIOCOMPOSITES

Hot Topics in Thermal Analysis and Calorimetry

Volume 4

Series Editor:
Judit Simon, *Budapest University of Technology and Economics, Hungary*

Thermal Properties of Green Polymers and Biocomposites

by

Tatsuko Hatakeyama

Otsuma Women's University,
Tokyo, Japan

and

Hyoe Hatakeyama

Fukui University of Technology,
Japan

Visit Springer's eBookstore at: http://ebooks.springerlink.com
and the Springer Global Website Online at: http://www.springeronline.com

Contents

Preface

In recent years, green polymers have received particular attention, since people have become more environmentally conscious. During the last fifty years, green polymers have sometimes been neglected compared to more high profile research subjects in academic and industrial fields. The authors of this book have continuously made efforts to investigate the properties, especially thermal properties, of green polymers and to extend their practical applications. Hence, the first half of this book is devoted to our results on fundamental research and the second half describes our recent research, mainly based on the authors' patents.

The authors are grateful to our long term friends; Professor Clive Langham, Nihon University, to whom we are especially grateful for his editorial advice, Professor Kunio Nakamura, Otsuma Women's University, Dr. Shigeo Hirose, National Institute of Advanced Science and Technology, Professor Shoichiro Yano, Nihon University, Professor Hirohisa Yoshida, Tokyo Metropolitan University, Dr. Francis Quinn, Loreal Co., Professor Masato Takahashi, Shinshu University, Dr. Per Zetterlund, Kobe University, and Dr. Mika Iijima, Yokkaichi University. We also wish to thank Ms. Chika Yamada for her helpful assistance.

As Lao Tse, the ancient Chinese philosopher said, "materials that look fragile and flexible, like water, are the original matters of the universe". The authors hope that green polymers on the earth continue to coexist with us in the long term incarnation of the universe.

Hyoe Hatakeyama
Tatsuko Hatakeyama

List of abbreviations

AFM	atomic force microscopy
AL	alcoholysis lignin (Alcel lignin)
ALPCL	alcoholysis lignin-based PCL
CA	cellulose acetate
CAPCL	cellulose acetate-based PCL
CG	coffee ground
CL	ε-caprolactone
CMC	carboxymethylcellulose
CellPCL	cellulose-based polycaprolactone derivatives
C_p	heat capacity
DABCO	1,4-diazobicyclo(2,2,2)octane
DBTDL	di-n-butyltin dilaurate
DEG	diethylene glycol
DMA	dynamic mechanical analysis
DMAc	N, N-dimethylacetoamide
DPPH	1,1-diphenyl-2-picrylhydrazyl
DS	degree of substitution
DSC	differential scanning calorimetry
DTA	differential thermal analysis
DTA-TG	differential thermal analysis-thermogravimetry
DTG	derivative thermogravimetry
DT_d	derivative thermal decomposition temperature
ESR	electron spin resonance
E_a	activation energy
E'	dynamic storage modulus

E''	dynamic loss modulus
FTIR	Fourier transform infrared spectrometry
Fru	fructose
GP	graft polyol (styrene- and acrylonitrile grafted polyether)
Glu	glucose
KL	kraft lignin
KLDPU	kraft lignin-based diethylene glycol type polyurethane
KLPCL	kraft lignin-based PCL
KLPPU	kraft lignin-based polyethylene glycol type polyurethane
KLTPU	kraft lignin-based triethylene glycol type polyurethane
LDI	lysine diisocyante
LS	lignosulfonate
LSDPU	lignosulfonate-based diethylene glycol type polyurethane
LSPCL	lignosulfonate-based polycaprolactone
LSPPU	lignosulfonate-based polyethylene glycol type polyurethane
LSTPU	lignosulfonate-based triethylene glycol type polyurethane
LTI	lysine triisocyante
LiCL	lithium chloride
Lig	lignin
LigPCL	lignin-based PCL
M	mass
MDI	diphenylmethane diisocyanate [poly (phenylene methylene) polyisocyanate
ML	molasses
MLP	molasses polyol
MR	mass residue
MWL	milled wood lignin
NCO/OH	isocyanate group/hydroxyl group ratio
NMR	nuclear magnetic resonance spectrometry
NaCS	Sodium cellulose sulfate
OHV	hydroxyl group value
PCL	polycaprolactone
PEG	polyethylene glycol
PEP	polyester polyol
PPG	poly(propylene glycol)
PSt	polystyrene
PU	polyurethane
PVA	poly(vinyl alcohol)
PVP	poly(vinyl pyroridone)
RH	relative humidity, %
SEM	scanning electron microscopy
Suc	sucrose

T	temperature
TBA	torsion braid analysis
TDI	tolylene diisocyanate
TEG	triethylene glycol
TG	thermogravimetry
TMA	thermomechanical analysis
TMAEP	trimethylaminoethylpiperazine
T_{cc}	cold-crystallization temperature
T_d	thermal degradation temperature
T_g	glass transition temperature
T_m	melting temperature
WAX	wide line x-ray diffractometry
W_c	water content= mass of water / mass of dry sample, $g\ g^{-1}$
$\tan \delta$	$=E''/E'$
ΔC_P	heat capacity difference at T_g
ΔH_m	enthalpy of melting
ε	strain
ρ	apparent density
σ	strength

Chapter 1

INTRODUCTION

1. OVERVIEW OF GREEN POLYMERS

Synthetic polymers are essential for modern human life, since they are used in industrial and agricultural fields. However, most synthetic polymers that have been developed by using petroleum and coal as raw materials are not compatible with the environment, since they cannot be included in the natural recycling system. There are serious contradictions between the convenience that people require today and compatibility with the natural environment. It is easy to say that we should use only natural materials in order to solve the problems coming from man-made materials. However, this means that we lose all the convenient features and materials which science has developed through human history. Therefore, development of environmentally compatible polymers (**green polymers**) is the key to sustainable developments that can maintain our rich and convenient life. Table 1-1 offers an overview of green polymers that have recently been developed.

In order to develop green polymers, it is essential to understand that nature constructs a variety of materials that can be used. Saccharides have already been used extensively in the food, medical and cosmetic industries. Plant materials such as cellulose, hemicellulose and lignin are the largest organic resources. However, it can be said that the above natural polymers, except for cellulose, are not very well used. Hemicellulose has not yet been utilized. Lignin, which is obtained as a by-product of the pulping industry is mostly burnt as fuel and only increases the amount of carbon dioxide in the environment, although lignin is one of the most useful natural resources.

Table 1-1. Examples of green polymers

Polymer types	Examples
From microorganisms	Polysaccharides such as xanthan gum, alginic acid, hyaluronan, and gellan gum
	Polyesters such as poly(hydroxyalkanoate)s
From plants	Polysaccharides such as cellulose, lignin, starch, carrageenan, and locust bean gum
	Cellulose esters such as cellulose acetates
	Saccharide-based polyurethanes and polycaprolactone derivatives
	Lignin-based polyurethanes and poly-caprolactone derivatives
	Starch-based blends
From animals	Collagen, Chitin
	Chitin and chitosan-based polymeric derivatives and composites

Biomaterials span the range from elastic solids to viscous liquids. However, they have been difficult to use as natural resources for polymers that are useful for human life because of the complexity based on the intricacies of their molecular architecture. However, scientific advances enable us to understand molecular features of biomaterials through modern analytical methods. Now it is the time to consider that the compounds produced through biosynthesis can be used as half-made up raw materials for the synthesis of useful plastics and materials. Major plant components, such as saccharides and lignin, contain highly reactive hydroxyl groups that can be used as reactive chemical reaction sites. As shown in Figure1-1, it is possible to convert saccharides and lignin to various green polymers that are environmentally compatible [1-26].
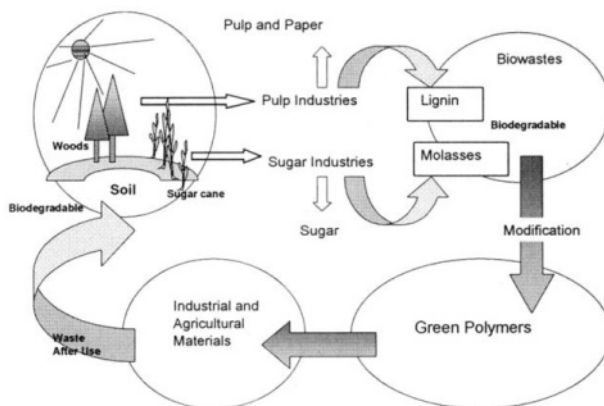

Figure 1-1. Circulation of lignin- and saccharide-based synthetic polymers in nature.

This book is concerned with the thermal properties of green polymers such as natural polymers and polymers derived from saccharides and lignins. The above green polymers include polymers such as poly(ε-caprolactone) (PCL) and polyurethane (PU) derivatives. PCL derivatives were synthesized from lignin, saccharides, cellulose and cellulose acetates. PU derivatives were prepared from saccharides and lignins. Thermal properties of the above polymers were characterized by various thermal analyses including thermogravimetry (TG), differential thermal analysis (DTA), differential scanning calorimetry (DSC), thermomechanometry (TMA) and dynamic mechanical analysis (DMA). Simultaneous measurements combining various techniques such as TG-Fourier transform-infrared spectrometry (FTIR) and TG-DTA are also mentioned.

2.   MOLECULAR LEVEL MORPHOLOGY OF IMPORTANT GREEN POLYMERS: CELLULOSE AND LIGNIN

The molecular architecture of cellulose and lignin has received particular attention for over 100 years, since both biopolymers are the major components of plant materials. Due to recent studies performed by x-ray diffractometry and solid state nuclear magnetic resonance spectrometry (NMR), the crystalline structure of cellulose has been investigated. In contrast, the higher-order structure of lignin in the amorphous state has scarcely been studied, since analytical methods were limited. The results were averaged over the number of molecules based on indirect analysis. Recently, the supermolecular structure of biopolymers has been investigaited in nano-level, since it is possible to observe individual molecules and molecular assemblies by atomic force microscopy (AFM) [27]. AFM directly visualizes the heterogeneity of biopolymers either in crystalline or amorphous state. Furthermore, morphological observation can be correlated with the results obtained by other physical measurements.

AFM has been used in order to observe the supermolecular structure of cellulose and lignin by using their water soluble derivatives such as sodium carboxymethylcellulose (NaCMC), sodium cellulose sulfate (NaCS) and sodium lignosulfonate (LS). Water soluble derivatives were used as samples, since aqueous solutions of samples were easy to spread on a freshly cleaved mica surface. The samples spread on mica were imaged by AFM.

An AFM image of NaCMC is shown in Figure 1-2. Rigid strands are clearly observed. The thickness of strands is ca. 0.7 nm, which strongly indicates that NaCMC molecules extended on mica surface are in mono- or

double layers.   It is considered that the hydrophobic side of molecules attaches to the mica surface and the carboxymethyl groups extend to the outer surface. The width of the strands ranges from 15.2 to 18.2 nm. When the results obtained by x-ray diffractometry are taken into consideration, 4 to 5 molecules are bundled and observed as a strand. In the above calculation, the size of the geometrical shape of the needle and the samples are calibrated. Figure 1-3 shows a three dimensional AFM image of NaCMC.
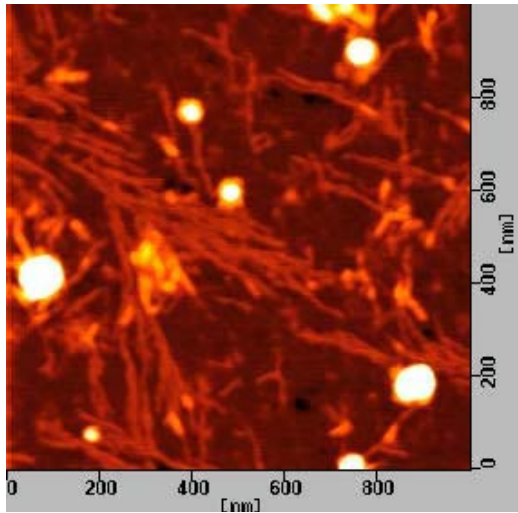

Figure 1-2. AFM image of sodium carboxymethylcellulose (NaCMC, concentration 10 µg ml^{-1}) showing extended molecular chain.
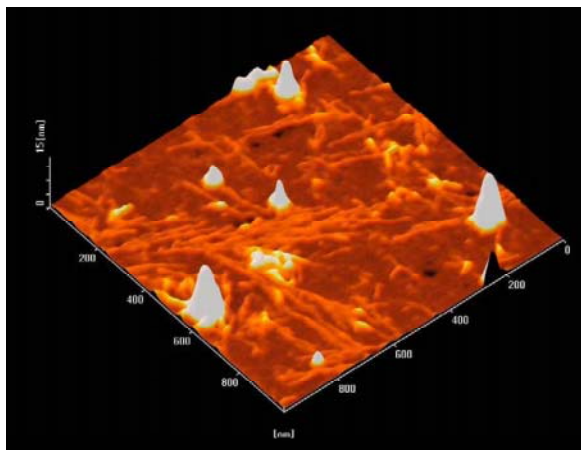

Figure 1-3. Three dimensional AFM image of NACMC (concentration 10 µg ml^{-1}).

Figures 1-4 and 1-5 show two and three dimensional AFM images of NaCS. Both figures indicate that sodium cellulose sulfate (NaCS) molecules show worm-like structures. The difference of the molecular shape between NaCMC and NaCS may be caused by the difference of substituted groups and also the degree of substitution (DS).
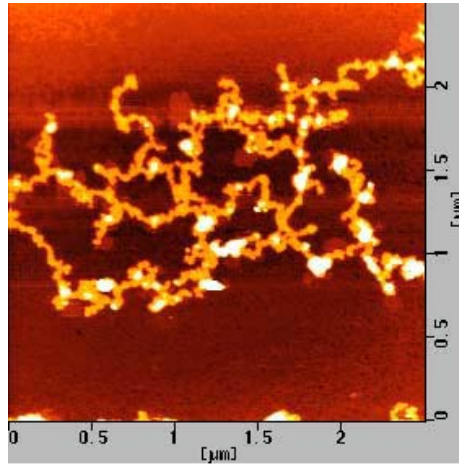

Figure 1-4. AFM image of sodium cellulose sulfate (NaCS) showing worm-like molecular chain structure (concentration 10 µg ml^{-1}).

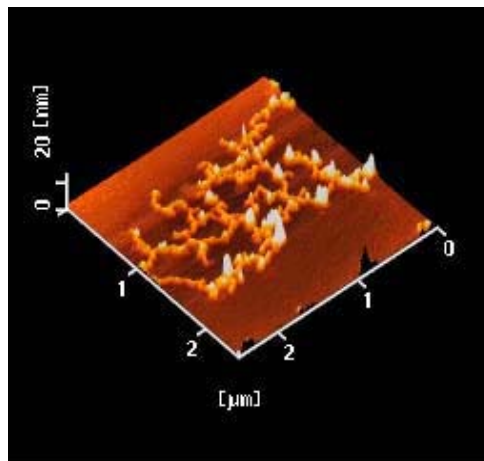*Figure 1-5.* Three dimensional AFM image of NaCS showing worm-like molecular chain structure (concentration 10 µg ml^{-1}).

Figures 1-6 and 1-7 show two and three dimensional AFM images of sodium lignosulfonate (NaLS). Both figures show that lignin has a complicated network structure that is highly crosslinked.
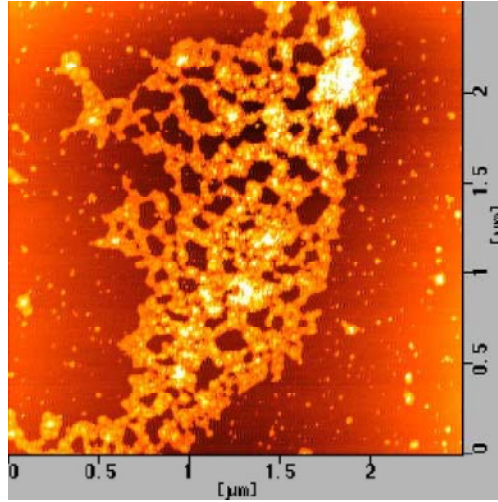

Figure 1-6. AFM image of sodium lignosulfonate (NaLS) showing molecular chain forming network structure (concentration 10 µg ml^{-1}).

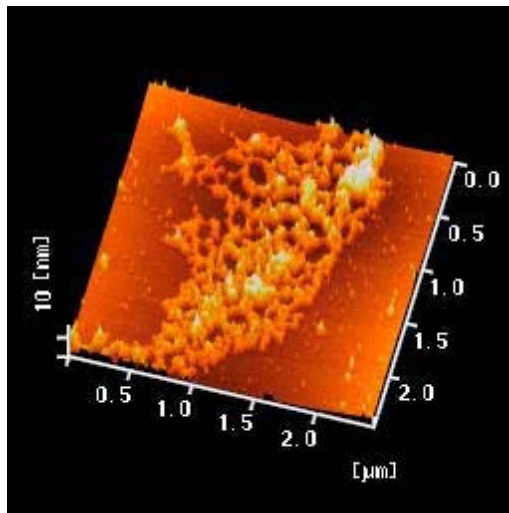*Figure 1-7.* Three dimensional AFM image of sodium lignosulfonate (NaLS) showing molecular chain forming network structure (concentration 10 µg ml^{-1}).

3. RAW MATERIALS FOR SYNTHETIC GREEN POLYMERS: MOLASSES AND LIGNIN

3.1 Molasses

Molasses is a brown viscous liquid and is produced from sugar cane and beet. The chemical components of molasses consist of sucrose and saccharides such as glucose and fructose. An example of the chemical components of molasses is shown in Table 1-2. Molasses is usually used as an ingredient in the fermentation industry and also for livestock feed. However, it has been found that it is useful as a raw material for the synthesis of saccharide-based polyurethanes and polycaprolactones [1-11]. Molasses from sugar cane is produced in tropical and subtropical regions such as Brazil, Cuba, Thailand, Indonesia, Philippines and Okinawa.

Table 1-2. Chemical components of molasses [26]

Chemical components	Content / %
Sucrose	32.5
Glucose	8.5
Fructose	9.2
Other Saccharides	2.3
Water	20.5
Ash	9.5

On the other hand, beet molasses is produced in cold regions such as northern Europe, Russia and Hokkaido, Japan. Recent sugar production in the world is ca. 130 million tons / year. Production of molasses corresponds to ca. 30 % of sugar production. Accordingly, it is considered that 40 million tons / year of molasses is produced in the world. This amount seems to be more than enough for the production of environmentally compatible bio-based polymers in the future.

3.2 Lignins

Lignins are derived from renewable resources such as trees, plants, and agricultural crops. About 30 % of wood constituents are lignin. Lignins are nontoxic and extremely versatile in performance. Most industrial lignins are obtained from kraft and sulfite pulping processes. Kraft lignin is usually burnt as fuel at pulping mills. Annual lignin production in Japan is estimated to be about 8 million tons. Lignin production in the world is approximately 30 million tons / year. However, it should be noted that this value is only an estimate, since there are no reliable statistics on lignin production because it is mostly burnt as a fuel immediately after production. About one million

tons of water soluble lignosulfonate derivatives which are by-products of sulfite pulping are consumed in Japan as chemicals such as dispersants [28].

Commercial lignin is a by-product of the pulping industry, as mentioned above, and is separated mostly from wood by a chemical pulping process. As described above, major delignification technolgies used in the pulping process are kraft and sulfite methods. Other delignification technologies are solvolysis processes using organic solvents or high pressure steam treatments to remove lignins from plants.

Since lignins are natural polymers with random crosslinkings, their physical and chemical properties differ depending on extraction processes. A part of the schematic chemical structure of lignin is shown in Figure 1-9.
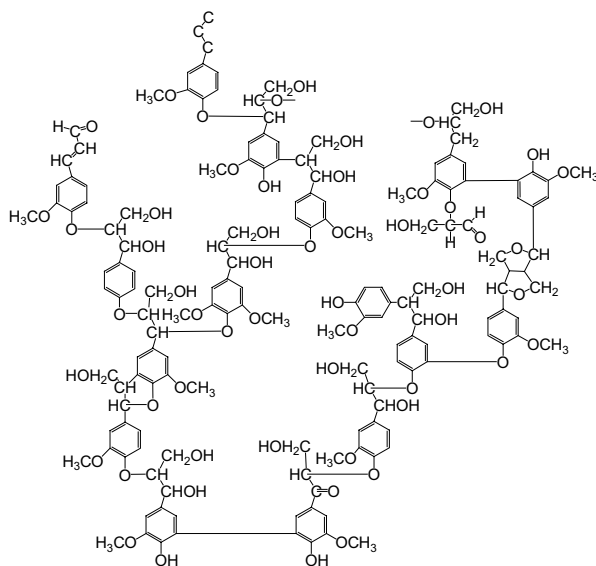

Figure 1-8. A part of schematic chemical structure of lignin [29].

As described in Chapter 5 of this book, the higher-order structure of lignin, which consists of phenyl propane units, is fundamentally amorphous. Three phenylpropaniod monomers such as coniferyl alcohol, synapyl alcohol and *p*-coumaryl alcohol are conjugated to produce a three dimensional lignin polymer in the process of radical-based lignin biosynthesis. For the above reason, lignin does not have a regular structure like cellulose, but is a physically and chemically heterogeneous material, although the exact chemical structure is unknown.

Since each lignin molecule has more than two hydroxyl groups, lignin-based polyurethane derivatives, polycaprolactone derivatives and epoxy

resins are obtainable by using the hydroxyl group as the reaction site [1,2, 12-26].

4. SCOPE OF THIS BOOK

This book is concerned with characterization of polymers such as cellulose, lignin and green polymers by thermal and mechanical analyses, spectroscopy, and x-ray diffractometry. Synthesis of green polymers derived from saccharides and lignins, such as polyurethane and polycaprolactone derivatives having saccharide and lignin structures in the molecular chain is also described.

This book consists of 8 chapters. In Chapter 1, " Introduction", the background and objectives of this book are introduced. Chapter 2 is concerned with various analytical methods that are useful for the characterization of green polymers. The analytical methods are thermal analyses, such as differential scanning calorimetry (DSC), thermogravimetry (TG) and TG-Fourier transform-infrared spectrometry (TG-FTIR), spectroscopy such as infrared spectroscopy and nuclear magnetic resonance spectroscopy (NMR), microscopy such as polarizing microscopy, scanning electron microscopy and atomic force microscopy, and x-ray diffractometry. Chapter 3 is devoted to the discussion of thermal properties of cellulose, cellulose-water interaction, liquid crystals from water-soluble cellulose derivatives and hydrogels. Chapter 4 is on hydrogels and liquid crystals of various polysaccharides. Chapter 5 concerns various properties of lignins. Chapter 6 is concerned with polycaprolactone derivatives having cellulose and lignin structures in the molecular chain. Chapter 7 deals with polyurethane derivatives from saccharides and lignin. Chapter 8 describes biocomposites containing plant and inorganic materials.

REFERENCES

1. Hatakeyama, H., 2002, Thermal analysis of environmentally compatible polymers containing plant components in the main chain. *J. Therm. Anal. Cal.,* **70**, 755-759.
2. Hatakeyama, H., Asano, Y. and Hatakeyama, T., 2003, Biobased polymeric materials. In *Biodegradable Polymers and Plastics* (Chellini, E. and Solario, R. eds.), Kluwer Academic / Plenum Publishers, New York, pp. 103-119.
3. Hirose, S. Kobashigawa K. and Hatakeyama, H. 1994, Preparation and physical properties o f polyurethanes derived from molasses. *Sen-i Gakkaishi*, **50**, 538-542.
4. Morohoshi, N., Hirose S., Hatakeyama, H., Tokashiki, T. and Teruya, K., 1995, Biodegradation of polyurethane foams derived from molasses. *Sen-i Gakkaishi*, **51**, 143-149.

5. Zetterlund, P., Hirose, S., Hatakeyama, T., Hatakeyama, H. and Albertsson, A-C., 1997, Thermal and mechanical properties of polyurethanes derived from mono- and disaccharides. *Polym. Inter.*, **42**, 1-8.

6. Hatakeyama, H., Kobahigawa, K., Hirose, S. and Hatakeyama, T., 1998, Synthesis and physical properties of polyurethanes from saccharide-based polycaprolactones. *Macromol. Symp.*, **130**, 127-138.

7. Hatakeyama, T., Tokashiki, T. and Hatakeyama, H., 1998, Thermal properties of polyurethanes derived from molasses before and after biodegradation, *Macromol. Symp.*, **130**, 139-150.

8. Hatakeyama, H., 2000, Adaptation of plant components in molecular of environmentally compatible polymers. *Petrotech*, **23**, 724-730.

9. Hatakeyama, H., 2001, Thermal properties of biodegradable polymers. *Netsu Sokutei*, **28**, 183-191.

10. Hatakeyama, H., 2001, Biodegradable polyurethane using saccharide and lignin. In *Practical Technology of Bio-degradable Plastics*, CMC, Tokyo, pp. 97-108.

11. Asano, Y., Hatakeyama, H., Hirose, S. and Hatakeyama, T., 2001, Preparation and physical properties of saccharide-based polyurethane foams. In *Recent Advances in Environmentally Compatible Polymers* (J. F. Kennedy, G. O. Philips, P. A. Williams and H. Hatakeyama eds.), Woodhead Publishing Ltd., Cambridge, UK, pp. 241-246.

12. Yoshida, H., Mörck, R., Kringstad, K. P. and Hatakeyama, H., 1990, Kraft lignin in polyurethanes. II. Effects of the molecular weight of kraft lignin on the properties of polyurethanes from a kraft lignin-polyether triol-polymeric MDI system. *J. Appl. Polym. Sci.,* **40**, 1819-1832.

13. Reimann, A., Mörck, R., Hirohisa, Y., Hatakeyama, H. and K. P. Kringstad, 1990, Kraft lignin in polyurethanes. III. Effects of the molecular weight of PEG on the properties of polyurethanes from a kraft lignin-PEG-MDI system. *J. Appl. Polym. Sci.*, **41**, 39-50.

14. Nakamura, K., Mörck, R., Reimann, A., Kringstad, K. P. and Hatakeyama, H., 1991, Mechanical properties of solvolysis lignin-derived polyurethanes. *Polymer for advanced technology*, **2**, 41-47.

15. Nakamura, K., Hatakeyama, T. and Hatakeyama, H., 1992, Thermal properties of solvolysis lignin-derived polyurethanes. *Polymer for advanced technology*, **3**, 151-155.

16. Hirose, S., Nakamura, K., Hatakeyama, H., Meadows, J., Williams, P. A. and Phillips, G. O., 1993, Preparation and mechanical properties of polyurethane foams from lignocellulose dissolved in polyethylene glycol. In *Cellulosics: Chemical, Biochemical and Materials* (J. F. Kennedy Williams P. A. and Phillips, G. O., eds.), Ellis Horwood Limited, Chichester, UK, pp. 317-331.

17. Nakamura, K., Hatakeyama, H., Meadows, J., Williams, P. A. and Phillips, G. O., 1993, Mechanical properties of polyurethane foams derived from eucalyptus kraft lignin, In *Cellulosics: Chemical, Biochemical and Materials* (J. F. Kennedy Williams P. A. and Phillips, G. O., eds.), Ellis Horwood Limited, Chichester, UK, pp. 333-340.

18. Hatakeyama, H., Hirose, S., Nakamura, K. and Hatakeyama, T. 1993, New types of polyurethanes derived from lignocellulose and saccharides, In *Cellulosics: Chemical, Biochemical and Materials* (J. F. Kennedy Williams P. A. and Phillips, G. O., eds.), Ellis Horwood Limited, Chichester, UK, pp. 525-536.

19. Hatakeyama, H., 1993, Molecular design of biodegradable plastics, *Kagaku to Seibutsu*, **31**, 308-311.

20. Hatakeyama, H., 1993, Biodegradable plastics derived from plant resources, *Mokuzai Kogyo*, **48**, 161-165.

21. Hatakeyama, H. and Hirose, S., 1994, Design of biodegradable materials. *Kogyo Zairyo,* **42**, 34-37.
22. Nakamura, K., Nishimura, Y., Hatakeyama, T. and Hatakeyama, H., 1995, Mechanical and thermal properties of biodegradable polyurethanes derived from sericin. *Sen-i Gakkaishi*, **51**, 111-117.
23. Tokashiki, T., Hirose, S. and Hatakeyama, H., 1995, Preparation and physical properties of polyurethanes from oligosaccharides and lignocellulose system. *Sen-i Gakkaishi*, **51**, 118-122.
24. Hirose, S., Kobashigawa, K. and Hatakeyama, T., 1996, Preparation and physical properties of biodegradable polyurethanes derived from the lignin-polyester-polyol system, In *Cellulosics: Chemical, Biochemical and Materials* (J. F. Kennedy Williams P. A. and Phillips, G. O., eds.), Ellis Horwood Limited, Chichester, UK, pp. 277-282.
25. Nakano, J., Izuta, Y., Orita, T., Hatakeyama, H., Kobashigawa, K., Teruya, K. and Hirose, S., 1997, Thermal and mechanical properties of polyurethanes derived from fractionated kraft lignin. *Sen-i Gakkaishi*, **53**, 416-422.
26. Hirose, S., Kobashigawa, K., Izuta, Y. and Hatakeyama, H., 1998, Thermal degradation of polyurethanes containing lignin structure by TG-FTIR. *Polymer International*, **47**, 1-8.
27. Bonnel, D., 2001, *Scanning Probe Microscopy and Spectroscopy, Second Edition*, Wiley-VCH, New York.
28. Machihara, A. and Kawamura, M., 2001, Recent utilization of lignin. In *Recent Advances in Technology for Wood Chemical* (G. Meshituka ed.), CMC, Tokyo, 127-137.
29. Lin, S. W. and Dence, C. W., 1992, Methods in Lignin Chemaistry, Spring Verlag, Berlin, pp. 3-16.

Chapter 2

CHARACTERIZATION OF GREEN POLYMERS

In this chapter, experimental techniques which are ordinarily used in investigation of green polymers and related compounds will briefly be introduced. Conformation of apparatuses, results and practical experimental conditions will be included. Apparatuses introduced here are commercially available and widely found in laboratories. Experimental conditions of thermal analysis are in a moderate temperature range in which green polymers are measurable.

1. THERMAL ANALYSIS

Thermal analysis is defined as an analytical experimental technique which investigates the physical properties of a sample as a function of temperature or time under controlled conditions. This definition is broad and the following techniques are referred to conventionally as thermal analysis, i.e. thermogravimetry (TG), differential thermal analysis (DTA), differential scanning calorimetry (DSC), thermomechanometry (TMA) and dynamic mechanical analysis (DMA). Recently, simultaneous measurements combining various techniques are widely used In this section, TG-DTA, TG-Fourier transform infrared spectroscopy (TG-FTIR), DSC, TMA and DMA will briefly be introduced. Detailed information is shown elsewhere [1-36].
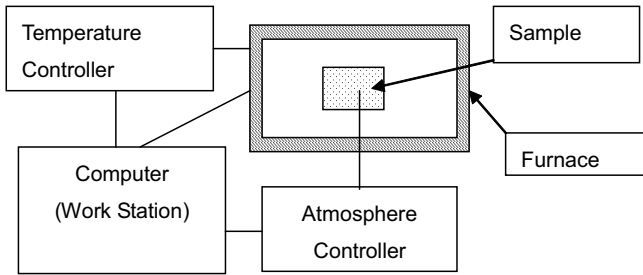
Figure 2-1. Conformation of thermal analysis apparatuses.

1.1 Thermogravimetry (TG)

1.1.1 TG-differential thermal analysis (DTA)

Thermogravimetry is the branch of thermal analysis which examines the mass change of a sample as a function of temperature in the scanning mode or as a function of time in the isothermal mode. A schematic conformation of a thermogravimeter is shown in Figure 2-2. At the present, almost all apparatuses used in the measurements of green polymers are those which enable simultaneous measurement of TG and differential thermal analysis (DTA) to be carried out. Balance systems, kinds of crucible, flow gas systems and other special attachments are described elsewhere in detail [6, 18, 32].
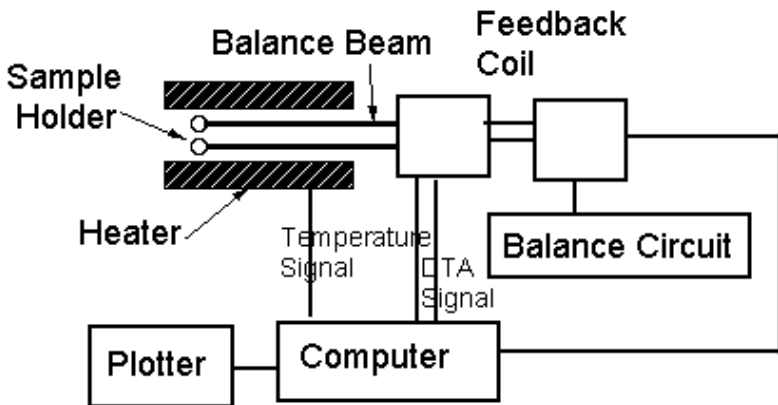

Figure 2-2. Schematic conformation of thermogravimeter.

In the investigation of green polymers, TG has been used in moderate conditions in order to obtain the following information.

1. Decomposition temperatures (T_{di}, T_d, T_{de}. etc)
2. Peak temperature of TG derivative curves (ΔT_{dp})
3. Mass residue at a temperature, range from 720 to 870 K (m_T)
4. Mass loss by vaporization of small molecular weight substances
5. Activation energy of decomposition and rate of decomposition

Standard TA computers are equipped with a software which determines the above basic results from (1) to (4). Additionally, a rate control program is commercially available [37, 38]. In order to measure green polymers, experimental conditions of TG which are ordinarily used in this book, are as follows; sample mass; 5 - 12 mg, material of crucible; platinium (carbon), shape of crucible: open and flat, temperature range; 290 - 870 K, heating rate (for standard measurements),10 - 20 K min^{-1}, heating rate (for calculation of kinetic parameters); 1 - 50 K min^{-1}, kinds of flow gas ; N$_2$, Air, or Ar (for special purpose), gas flow rate; 50 - 100 ml min^{-1}, respectively. Accuracy of data obtained by TG is found elsewhere [39]. Schematic TG curve and derivative curve are shown in Figure 2-3. T_d, ΔT_d, m_T are indicated using arrows. When two step decomposition is observed, the T_d is numbered from the low to high temperature side.
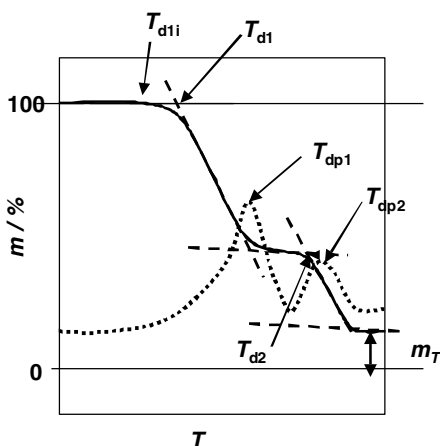

Figure 2-3. Schematic TG and TG derivative curves.

By using TG-FTIR, gases evolved from the sample decomposed in a TG sample cell are directly introduced to a FTIR sample cell and IR spectra are simultaneously measured as a function of temperature. In order to operate

this apparatus properly, it is important to control the temperature of the transfer tube connecting TG with FTIR. Evolved gases condense in the tube if the temperature is low, at the same time, secondary decomposition takes place if the temperature is too high. Temperature and flow rate of purging gas of the connecting tube must be controlled appropriately. Various kinds of natural polymers have been measured by TG-FTIR, such as lignin [33, 40], polyurethane derived from saccharides [41] and polycaprolactone grafted cellulose acetate [42]. Based on the TG-FTIR data, the decomposition mechanism of green polymers has been investigated. Representative FTIR curves obtained by TG-FTIR are shown in Figure 2-4.

Experimental conditions for standard measurements of green polymers by TG-FTIR are as follows; sample mass; 5 -10 mg, heating rate; 10 or 20 K min^{-1}, gas flow rate; 100 ml min^{-1}, temperature range; 290 - 870 K. temperature of connecting tube; 520 K, resolution of FTIR; 1 cm^{-1} and acquisition time 10 scan sec^{-1}, respectively.
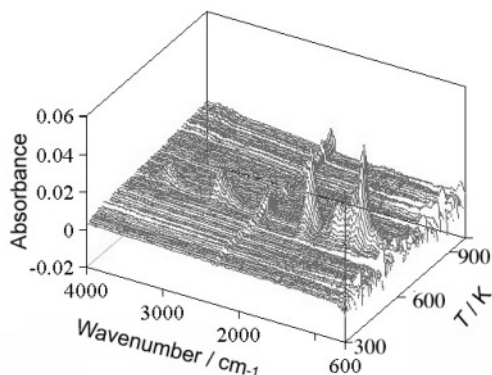

Figure 2-4. Three dimensional IR spectra as functions of wave numbers and temperature.

1.2   **Differential scanning calorimetry (DSC)**

Two types of DSC, power compensation type and heat flux type are used. In the power compensation type DSC, if a temperature difference is detected between the sample and reference, due to a phase change in the sample, energy is supplied until the temperature difference is less than a threshold value. In heat flux type DSC, the temperature difference between the sample and reference is measured as a function of temperature or time, under controlled temperature conditions. The temperature difference is proportional to the change in the heat flux.

When commercially available apparatuses of both types of DSC are compared, no large differences can be found concerning sensitivity, necessary amount of sample, temperature range of measurement, atmospheric gas supply, etc. Major differences between the two types of DSC are as follows; (1) due to the size of heater, isothermal measurements are easily carried out, when a power compensate type DSC is used. (2) due to the conformation of the sample cell, the low temperature measurements are carried out at a slow scanning rate, and a more stable baseline can be obtained by heat-flux type DSC.

Figure 2-5 shows a schematic conformation heat-flux type DSC and Figure 2-6 shows that of power compensation type DSC. Experimental conditions for standard measurements of green polymers by DSC are as follows; sample mass; 1 - 15 mg (ordinal condition, 5 - 7 mg), material of sample pan; Al (for solid and solution samples) and Ag (for dilute solution or hydrogels), shape of sample; open and flat type (for dry samples) and two different sealed types (for wet samples, solutions and hyrogels), temperature range; 120 K to a predetermined temperature lower than thermal decompositions (in standard conditions lower than 500 K), heating rate; 1 - 50 K min^{-1} (in standard conditions 10 K min^{-1}), atmospheric gas; N_2, gas flow rate; 30 ml min^{-1}. Repeatability and accuracy of DSC data of polymers are found elsewhere [43-45].
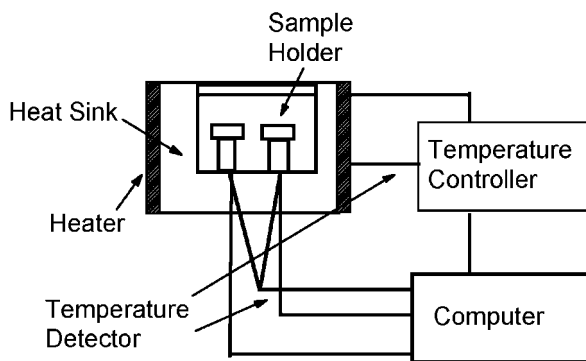

Figure 2-5. Schematic conformation of heat-flux type DSC.

By DSC, the following information on green polymers and related compounds is obtained.

1. The first order phase transition temperatures
2. Melting temperature (T_m)
3. Liquid crystal to liquid transition temperature (T_{lc-l})
4. Crystal to crystal transition

5. Crystallization temperature (T_c)
6. Cold crystallization temperature (T_{cc})
7. Pre-melt crystallization temperature (T_{pmc})
8. Liquid to liquid crystallization temperature ($T_{1\text{-}lc}$)
9. Glass transition temperature (T_g)
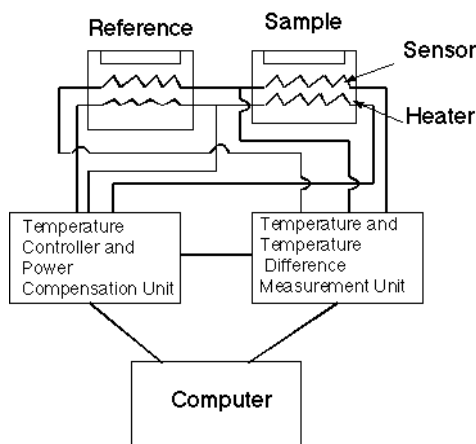10. Heat capacity difference at T_g (ΔC_p)

Figure 2-6. Schematic conformation of power compensation type DSC.

Figure 2-7 shows schematic DSC curves for the determination of transition temperatures and enthalpies. Ordinarily, peak temperature of melting (T_{pm}) and crystallization (T_{pc}) are used as an index of melting or crystallization temperature. It is noted that both temperatures are not obtained by equilibrium conditions. On this account, in this book the scanning rate is always shown in the figure captions. Scanning rate dependency of melting or crystallization of polymers is found elsewhere [29, 32].

Figure 2-8 shows a typical DSC heating curve of amorphous polymer. Glass transition is observed as a baseline deviation toward endothermic direction (direction of heat capacity increase). Due to the thermo-dynamically non-equilibrium nature of the glassy state, glass transition temperature (T_g) depends on the thermal history of a sample and measurement conditions such as the heating rate. On this account, the T_g value should always be stated along with precise experimental conditions and thermal history of the samples. In Figure 2-8, starting temperature (T_{ig}'), extrapolated temperature (T_{ig}), mid temperature (T_{mg}) and final temperature (T_{eg}) can be read. Generally T_{ig} or T_{mg} is reported as T_g. The above facts suggest that reported T_g values are not concrete values but

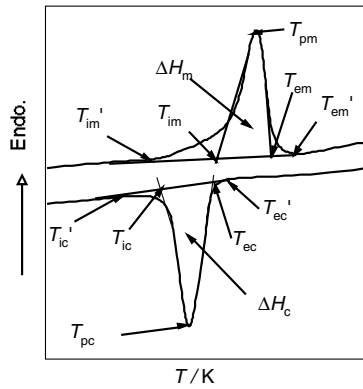depend on experimental conditions and definition of T_g.

Figure 2-7. Schematic DSC curves for the determination of transition temperatures and enthalpies.
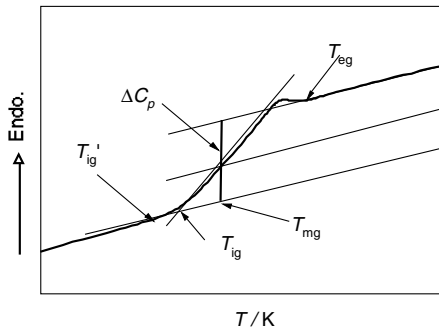

Figure 2-8. Schematic DSC heating curve showing glass transition. starting temperature (T_{gi}'), extrapolated temperature (T_{gi}), mid temperature (T_{gm}), final temperature (T_{gf}), heat capacity difference at T_{gi} (ΔC_p).

1.3 Thermomechanometry (TMA)

In thermomechanometry (thermomechanical analysis, TMA) the deformation of materials under constant stress, or constant strain, is measured as a function of temperature or time. Stress or strain can be applied to the sample in either a static or dynamic mode. Sample probes capable of measuring samples not only in air or inert gas but also in humid conditions or in water have been developed. A schematic conformation of a thermomechanometer is shown in Figure 2-9.

The following information can be obtained by static measurements of green polymers.

1. Glass transition temperature
2. Linear expansion or compression coefficient
3. Stress relaxation as a function of time at a predetermined temperature
4. Creep as a function of time at a predetermined temperature
5. Swelling rate and equilibrium swelling ratio under various stresses
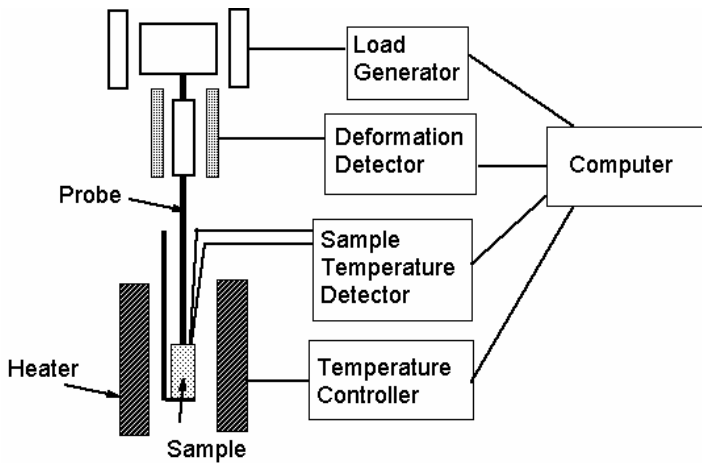6. Dynamic modulus, dynamic loss modulus and tan δ as a function of temperature.

Figure 2-9. Schematic conformation of a thermomechanometer.

Softening temperature measured by TMA is practically used in commercial and industrial fields. Softening temperature is neither glass transition nor melting, but at a temperature higher than "softening temperature" thermoplastics start to flow. On this account, the softening temperature is an important index for polymer processing. Repeatability and reliability of TMA data is confirmed by a round robin test [46]. Almost all green polymers in the solid dry state lack flowability. On this account, in this book, softening temperature will not be described. Experimental conditions for standard measurements of green polymers by TMA are as follows; probe material; quartz, temperature range; 290 - 520 K (for dry sample), 273 - 263 K (for hydrogels). Applied stress, strain and frequencies have a wide range according to the kind of sample and shape of probe. Although there are various shapes of probe, two kinds of probe were used as shown in Figure 2-10.

Typical TMA curves in compression mode are shown in Figure 2-11. Transition temperature is determined as a cross point of two extrapolated lines as shown in the figure.
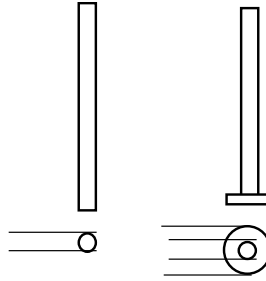

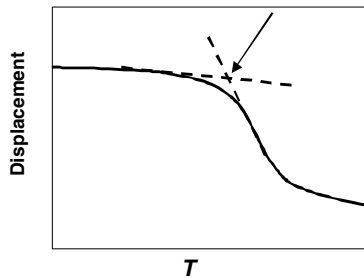*Figure 2-10.* TMA probes used in the experiments shown in this book.

Figure 2-11. Schematic TMA curve in compression mode.

The sample holder for the measurement of swelling of samples is shown in Figure 2-12 [47]. The sample sheet was placed on a quartz plate and predetermined stress applied. Water is supplied from the bottom via a flexible tube. Deformation is detected as a function of time. When temperature dependency of swelling is measured, a water bath whose temperature is controllable was connected to the sample probe. Temperature was changed stepwise.

Dynamic modulus (E') and dynamic loss modulus (E'') of hydrogels are measured using a TMA. A sample holder of TMA and schematic TMA curves of hydrogel applied sinusoidal oscillation in water are shown in Figure 2-13. Gel sample is dipped in water using a sample holder shown in A in Figure 2-13. Frequency ranges from 0.01 to 20 Hz. Applied stress depends on rigidity of gel. Ordinarily, ca. 1 x 10^3 Pa is applied. Measurements are carried out for several minutes at each temperature. From